Long-Range Effects in Liganded Hemoglobin Investigated by Neutron and UV Raman Scattering, FTIR, and CD Spectroscopies

Olivier Sire,[†] Christian Zentz,[†] Serge Pin,[†] Laurent Chinsky,[‡] Pierre-Yves Turpin,[‡] Pierre Martel,[§] Patrick T. T. Wong,[⊥] and Bernard Alpert*,[†]

Contribution from the Laboratoire de Biologie Physico-Chimique, Université Paris 7, 2 place Jussieu, 75251 Paris cedex 05, France, Laboratoire de Physico-Chimie Biomoléculaire et Cellulaire, CNRS UA 2056, Université Paris 6, 4 place Jussieu, 75252 Paris cedex 05, France, Atomic Energy of Canada Limited, Chalk River Laboratories, Chalk River, Ontario K0J 1J0, Canada, and University of Ottawa, Faculty of Medicine, 451 Smyth, Ottawa, Ontario K1H 8M5, Canada

Received February 4, 1997. Revised Manuscript Received August 7, 1997[⊗]

Abstract: The numerous investigations that have focused on the iron binding site to explain the different affinity of hemoglobin for CO and O_2 are still without success. Thus, this work addresses the problem of nonlocal effects, which have been disregarded so far. We have investigated the protein behavior in relation to the iron−ligand nature. The present data show that different parts of the protein, which are not in close contact with the heme pocket, are effectively influenced by the nature of the iron−ligand bond. Whereas oxyhemoglobin and carbonmonoxide hemoglobin in solution exhibit the same molecular shapes and helical contents, different electrostatic interactions in association with a redistribution of the strains occur in the protein matrix. Due to electric couplings of the heme to the protein, the whole molecule is sensitive to the chemical nature of the iron−ligand bond. This suggests that long distance electrostatic interactions promote the energy transduction through the protein molecule.

Introduction

Heme models have intrinsically higher affinity (30000- to 100000-fold) for carbonmonoxide (CO) than for oxygen (O_2). That the ratio decreases to approximately 200 in hemoglobin[1] emphasizes the specific role of the protein matrix. Nevertheless, X-ray crystallographic studies having shown that carbonmonoxide hemoglobin (HbCO) and oxyhemoglobin (HbO_2) maintain identical quaternary structure,[2,3] the origin of the affinity difference has been thought to lie in the iron-ligand bond geometry (ref 4 and articles therein, also ref 5), and more recently, has been related to polar and steric effects in the heme pocket.[6,7] Indeed, the most recent literature deals with site-directed mutagenesis studies which examine the role played by proximal and distal histidine residues in hemoprotein affinity. However, unequivocal evidence is still lacking,[6,7] and the basis for the affinity variations could be quite complex. Given the influence of protein matrix on the CO/O_2 affinity ratio, domains remote from the heme pocket should also be involved in determining the affinity of hemoglobin for its ligands, thus implicating nonlocal events which have been ignored until now. Therefore, we have searched for the repercussions on the whole protein molecule brought about by the iron-ligand nature: O_2 or CO. Possible differences in the molecular shapes of the two hemoglobin derivatives in solution were investigated by neutron scattering.[8] Secondary structure variations were observed with far-UV circular dichroism.[9] Infrared spectroscopy of the amide I′ band was employed to probe for hydrogen bond rearrangements within protein,[10] and changes in the electric field in the protein matrix were explored by UV resonance Raman studies of aromatic tyrosinyl (Tyr) and tryptophanyl (Trp) residues.[11]

Experimental Section

Samples. Human hemoglobin was extracted from red blood cells[12] and then stripped on an AG-501 resin (Bio-Rad).[13] H−D exchange (for infrared and neutron scattering measurements) was achieved by mixing 10 mL of 20 mM hemoglobin (concentration expressed on heme basis) with 100 mL of D_2O, followed by a vacuum concentration back to 20 mM. This procedure was repeated three times. After a centrifugation at 45 000 g, the protein solution was buffered (0.1 M bis-Tris, pD or pH 7) and converted to deoxyhemoglobin (deoxyHb) or HbCO by flowing pure N_2 or CO gases over the HbO_2 solution. Complete ligation of CO or O_2 or ligand loss (deoxy form) was checked by optical absorption (450−650 nm) by using a cell with an 8 μm path length. Methemoglobin (metHb) was produced by adding ferricyanide. Each of the techniques used in the present study requires a particular protein concentration ranging between 0.4 and 9 mM. Over this concentration domain, the tetramer molecule predominates, and it was assessed that no aggregation occurs. Before and after experiments,

[†] Laboratoire de Biologie Physico-Chimique, Université Paris 7. Tel: (331) 44 27 47 38. Fax: (331) 44 27 69 95. e-mail: bea@ccr.jussieu.fr.
[‡] Laboratoire de Physico-Chimie Biomoléculaire et Cellulaire, CNRS UA 2056, Université Paris 6.
[§] Atomic Energy of Canada Limited, Chalk River Laboratories.
[⊥] University of Ottawa.

[⊗] Abstract published in *Advance ACS Abstracts,* November 15, 1997.

(1) Antonini, E.; Brunori, M. In *Hemoglobin and myoglobin in their reactions with ligands;* North-Holland: Amsterdam, 1971; pp 263−264.
(2) Baldwin, J. *J. Mol. Biol.* **1980,** *136*, 103−128.
(3) Shaanan, B. *J. Mol. Biol.* **1983**, *171*, 31−59.
(4) Collman, J. P.; Brauman, J. I.; Doxsee, K. M. *Proc. Natl. Acad. Sci. U.S.A.* **1979,** *76*, 6035−6039.
(5) Traylor, T. G.; Berzinis, A. P. *Proc. Natl. Acad. Sci. U.S.A.* **1980**, *77*, 3171−3175.
(6) Ray, G. B.; Li, X. Y.; Ibers, J. A.; Sessler, J. L.; Spiro, T. G. *J. Am. Chem. Soc.* **1994**, *116*, 162−176.
(7) Springer, B. A.; Sligar, S. G.; Olson, J. S.; Phillips, G. N. *Chem. Rev.* **1994**, *94*, 699−714.
(8) Martel, P.; Kim, S. M.; Powell, B. M. *Biophys. J.* **1980**, *31*, 371−380.
(9) Manning, M. C.; Illangasekare, M.; Woody, R. W. *Biophys. Chem.* **1988**, *31*, 77−86.
(10) Byler, D. M.; Susi, H. *Biopolymers* **1986**, *25*, 469−487.
(11) Demchenko, A. P. In *Ultraviolet Spectroscopy of Proteins;* Springer-Verlag: Berlin, 1986; pp 137−144.
(12) Perutz, M. F. *J. Cryst. Growth* **1968**, *2*, 54−56.
(13) Jelkmann, W.; Bauer, C. *Anal. Biochem.* **1976**, *75*, 382−388.

S0002-7863(97)00378-8 CCC: $14.00

samples were checked spectrophotometrically with a Varian or Beckman UV−visible spectrophotometer. No evidence for photochemical damage, iron oxidation, or protein denaturation was observed subsequent to the experiments.

Neutron Scattering. A neutron beam (34.2 meV) was provided by the nuclear reactor at Chalk River (Ontario, Canada). Neutron scattering measurements were carried out at 20 °C, in the high angle region of the "small angle neutron scattering" (SANS) regime,[14] where information about the molecular shape can be obtained.[8,15] SANS protein data were corrected from the buffer signal and for the non-uniformity of the detector response by normalization of the incoherent scattering to that of a 5 mm thick D_2O sample. Each measurement was made on ≅9 mM of protein (150 mg/mL) with an acquisition time of 8 h and a neutron wavelength of $\lambda = 0.1533$ nm.

Circular Dichroism. CD spectra were collected by using a Jobin Yvon Mark V dichrograph over the 190 to 260 nm range that provides a signal extremely sensitive to small secondary conformational distortions.[9] Pure dry N_2 gas (12 L/min) was continuously flushed through the apparatus. Each experiment was the average of five successive scans (2-nm bandwidth) encoded with a 0.5-nm step. Each spectrum (0.93 mM in heme) results from four independent experiments at 20 °C in a Hellma cell, with an 8-μm optical pathlength. Over the whole wavelength domain investigated, the baseline drift was within 2−3%. Hence, experimental optical activity variations larger than 6−7% must be considered as significant. Data are expressed in term of molecular ellipticity (deg·cm^2·dmol^{-1}).

Fourier Transform Infrared Spectroscopy. Infrared spectra were recorded with either a 10 MX Nicolet or a Bomem Michelson 110 Fourier transform spectrophotometer equipped with a liquid-N_2-cooled HgCdTe detector. Samples (6 mM of protein at 20 °C) were placed in an infrared cell with CaF_2 or BaF_2 windows and a path length of 50 or 25 μm. Scan duration was optimized to get a good signal/noise ratio without introducing band distortion that may arise from source drifts. Solvent contribution was removed by subtracting the deuterated buffer spectrum from that of the protein solution. This subtraction (achieved over the 2000−1400 cm^{-1} wavenumber domain) yields a flat baseline on the 2000−1750 cm^{-1} wavenumber domain. Data treatment was performed with software developed in Ottawa,[16] which allows the contribution from the water vapor to be interactively subtracted. The IR amide I′ band (the most useful for studying the H-bond distribution within the protein[10]) was normalized in terms of protein concentration by measuring directly the OD value in the visible domain on the FTIR cell.

Band narrowing was achieved by Fourier self-deconvolution.[17] The second derivative of the spectrum was used to determine the number and position of the different components.[18] Amide I′ band contour was described as the sum of these different components, and their relative areas were assumed to be proportional to the amount of the various types of structures.[17,19]

UV Raman Spectroscopy. The experimental setup is described in ref 20. The UV resonance Raman (UVRR) signals of the protein aromatic residues were acquired with a monochannel Jobin-Yvon HG2S double monochromator working in the second order of the gratings and a solar-blind photomultiplier. Spectral slit width was set to a rather larger value, leading to a ±3 cm^{-1} accuracy in the band position, to allow a reasonable Raman signal to be analyzed while the laser excitation energy was limited to the lowest possible value to be able to reach a suitable Raman signal/noise ratio. The Raman excitation light (223.6 nm) was provided by a Datachrom 5000 dye laser (100−200 μJ per pulse) by using a Nd-YAG source (pulse duration 20 ns) with a low repetition rate of 10 Hz.

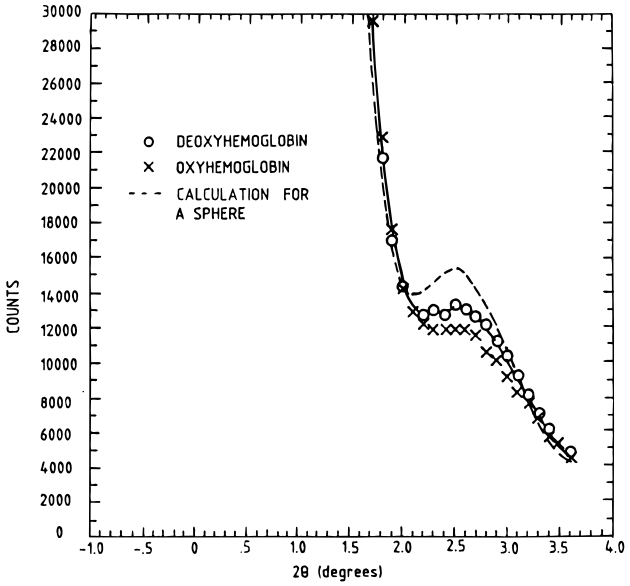

Figure 1. Neutron scattering spectra of human deoxy- and oxyhemoglobins in solution. Spectra of HbO_2 and HbCO are identical. Models assuming that the shape of the molecules can be described by a general ellipsoid (open circles and crosses) are clearly better than those corresponding to a spheroid (broken line). The semi-axes values corresponding to the best fits are given in Table 1. Error bars are smaller than the size of the dots. Experimental conditions are as follows: 0.1 M bis-Tris, pD 7; protein concentration 150 mg/mL; 20°C.

The low laser energy minimizes the risks of generating photodamage often induced by high-power UV pulsed excitation[21] and producing some photodeligated hemoglobin. To avoid the detection of a few photodeligated hemoglobin molecules, the samples were continuously stirred with a small magnet. This procedure brings down the low probability for two successive photons to hit, during the same laser pulse, the same hemoglobin molecule in the sample. Thus, any photodeligated species produced during the time of the laser pulse is unable to produce the Raman scattering effect. In the case of HbCO, the sample was highly saturated with CO to accelerate the CO religation of the small amount of deoxyHb photoproduct if any. The pulse repetition rate being low enough, the hemoglobin CO religation is totally finished before the arrival of another laser pulse. Therefore, the low laser energy, the high CO concentration, and the low pulse repetition rate are the dominant factors used to discard any transient deoxyHb signal that can contaminate the Raman scattering spectra of the photolabile HbCO species.

Each Raman spectrum (from 0.4 mM of protein) was averaged over six scans, and normalized on the large water O−H stretching band located around 3450 cm^{-1}.

Results

SANS Measurements. Even in the absence of the structural difference between HbO_2 and HbCO in their crystal state, the protein in an aqueous solution may exhibit different molecular shapes depending on the iron-ligand nature. Possible changes in the molecular dimensions have been sought by neutron scattering measurements in the high angle region of the SANS regime.[14] In this region, coherent intensity scattered by the macromolecules allows the protein to be described in terms of spheroids of various shapes.[8,14,15] Figure 1 presents the number of counts of the coherent intensity scattered by the protein *vs* the scattering angle 2θ. To compare with results in the literature, which are plotted as a function of the modulus Q of the transfer wavevector, Q can be calculated from the neutron wavelength ($\lambda = 0.1553$ nm) and the scattering angle 2θ by using the equation:

(14) Mittelbach, P.; Porod, G. *Acta Phys. Austriaca* **1962**, *15*, 122−147.
(15) Glandieres, J. M.; Calmettes, P.; Martel, P.; Zentz, C.; Massat, A.; Ramstein, J.; Alpert, B. *Eur J. Biochem.* **1995**, *227*, 241−248.
(16) Kauppinen, J. K.; Moffatt, D. J.; Mantsch, H. H.; Cameron, D. G. *Appl. Spectrosc.* **1981**, *35*, 271−276.
(17) Cameron, D. G.; Moffatt, D. J. *Appl. Spectrosc.* **1987**, *41*, 539−544.
(18) Dong, A.; Huang, P.; Caughey, W. S. *Biochemistry* **1990,** *29*, 3303−3308.
(19) Surewicz, W. K.; Mantsch, H. H. *Biochim. Biophys. Acta* **1988**, *952*, 115−130.
(20) El Antri, S.; Sire, O.; Alpert, B.; Turpin, P.-Y.; Chinsky, L. *Chem. Phys. Lett.* **1989**, *164*, 45−49.
(21) Asher, S. A.; Ludwig, M.; Johnson, C. R. *J. Am. Chem. Soc.* **1986**, *108*, 3186−3197.

Table 1. Calculated Parameters of the Molecular Shape of Hemoglobin Derivatives[a]

sample	*a* (Å)	*b* (Å)	*c* (Å)	model vol (Å^3)	χ^2
human Hb	26.6 ± 1.0	27.2 ± 1.0	32.7 ± 0.1	99100 ± 7800	1.19
horse deoxyHb*	26.5	26.5	35.5		
human HbO_2	29.9 ± 0.9	31.3 ± 1.1	24.2 ± 0.1	95700 ± 6000	2.19
horse HbO_2*	27.5	32.0	25.0		
human HbCO	29.7 ± 0.4	31.8 ± 0.5	24.1 ± 0.1	95300 ± 6500	0.94
human MetHb	29.9 ± 0.7	32.3 ± 0.9	24.4 ± 0.1	98700 ± 5500	3.06

[a] Data (identified with an asterisk) from horse hemoglobin[22,23] are displayed for comparison between neutron scattering and X-ray cristallography techniques. Calculations assuming oblate ellipsoids gave χ^2 values better than those obtained from a model involving ellipsoids of revolution.

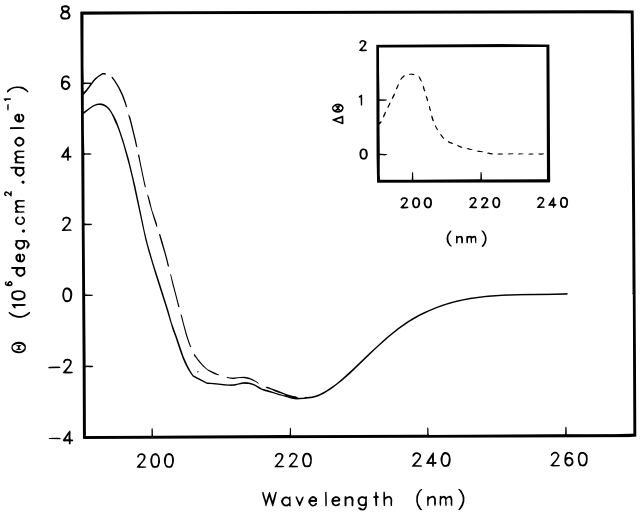

Figure 2. Iron−ligand effect on the far-UV CD spectrum of human hemoglobin. Experimental spectra: solid line, HbO_2; broken line, HbCO. Inset: Spectrum of HbCO *minus* HbO_2. The profile of this difference spectrum is typical of a β turn type II. $\Delta\Theta$ has the same unit as Θ. Experimental conditions are as follows: 20 °C; 0.1 M bis-Tris, pH 7; protein concentration 0.93 mM; optical path length 8 μm.

$$Q = 4\pi\lambda^{-1} \sin\theta$$

A protein description in terms of an ellipsoid with *a*, *b*, and *c* semiaxes was used to fit the coherent intensity scattered. The figure shows that the side peak centered around 2.5° is more pronounced in the case of a sphere (broken line), and decreases on going to deoxyHb and then to HbO_2. Semiaxes values are displayed in Table 1. Data from X-ray crystallography[22,23] have been given for comparison. The agreement is quite satisfactory. Changes are only observed between the deoxy form and any other form: HbO_2 and HbCO exhibit identical molecular shapes.

Far-UV CD Measurements. Circular dichroism is extremely sensitive to small distortions:[9] subtle rearrangements in the secondary structure of HbO_2 and HbCO were investigated over the 190−260 nm UV CD domain. Figure 2 presents the far-UV CD spectra of HbO_2 and HbCO. Significant differences occur in the 225−190 nm domain. The differential spectrum (HbCO-HbO_2) indicates that some βII turns[24] are influenced by the iron−ligand change. As crystallographic studies have clearly shown that the number of turns is identical for both HbO_2 and HbCO,[2,3] the pattern of the differential UV CD signal (inset of figure 2) points out that HbCO contains more constrained turns than HbO_2.

Infrared Amide I′ Band Measurements. Since the iron−CO ligation results in stiffer strains on turns, this should be revealed in the infrared amide I′ band. Indeed, the shape, intensity, and position of this band depend on the main chain hydrogen bonds involving C═O and N−H peptide groups evenly distributed within the protein.[25] Figure 3 displays the experimental and deconvoluted amide I′ band of HbO_2, HbCO, and Hb. From the shape of this band, it appears that the H-bond network is rearranged subsequent to the iron-ligation change. The energy distribution of the H bonds is less homogeneous in HbO_2 than in HbCO. Figure 3 also shows the second derivative spectra of HbO_2 and HbCO with the position of their various structural components. The component located at 1672 cm^{-1} corresponds to β-turn types I and II.[10,26] The peak around 1635 cm^{-1} is most likely due to H bonds linking different helical cylinders.[10,27] Most probably, the component located around 1615−1619 cm^{-1} results from interactions between subunits, these molecular interactions occurring between non-aggregated molecules.[28] To obtain more quantitative information, the area of each component was calculated. Data confirm that the α-helix (peak at 1654 cm^{-1}), as expected, is the dominant structure[29] and that the helical content is not sensitive to the iron−ligand nature. The HbCO/HbO_2 ratio for each component area can be used as an index for the rearrangement within the H-bond lattice, which would occur subsequent to the iron−ligand change. Table 2, which presents these HbCO/HbO_2 ratios, clearly shows the change in the distribution of strains over the intersubunit contacts and the chain−chain interactions, as well as the tensions on the turns of the protein.

Table 2. Area Ratio HbCO/HbO_2 of IR Amide I′ Band Components[a]

components (cm^1)	1615−1619	≅1635	1654	1672
assignment	subunits interaction	helix−helix	α-helix	β-turn
HbCO/HbO_2 ratio	0.77	1.16	1	1.14

[a] Band intensities and widths were estimated from the χ^2 hypersurface.[49] Error level ≅ 3−5%.

UVRR Measurements. UV resonance Raman spectra of hemoglobin have been collected with respect to the nature of the iron−ligand bond. Owing to their polarizability properties, the aromatic amino acid residues of the protein exhibit Raman line intensities and wavenumbers which are sensitive to structural rearrangements, local variation of the dielectric constant, and the electrostatic interactions within the protein matrix.[11,30,31] Figure 4 displays UVRR spectra of HbO_2 and HbCO. The pattern of the UVRR signal of the deoxyHb is presented, for comparison, in the inset of the same Figure 4. As expected, spectra are dominated by the vibrational contributions from Trp and Tyr residues[20,31,32] and essentially no heme contribution. Trp residues contribute to the band around 762

(22) Bragg, L.; Howells, F. R. S.; Howells, E. R.; Perutz, M. F. *Proc. R. Soc.* **1954,** *A 222*, 33−44.
(23) Perutz, M. F. *Proc. R. Soc*. **1969**, *B 173*, 113−140.
(24) Perczel, A.; Fasman, G. D. *Protein Sci.* **1992**, *1*, 378−395.
(25) Miyazawa, T.; Shimanouchi, T.; Mizushima, S. I. *J. Chem. Phys*. **1956**, *24*, 408−418.
(26) Krimm, S.; Bandekar, J. *Biopolymers* **1980**, *19*, 1−36.
(27) Le Tilly, V.; Sire, O.; Alpert, B.; Wong, P. T. T. *Eur. J. Biochem*. **1992**, *205*, 1061−1065.
(28) Clark, A. H.; Saunderson, D. P. H.; Suggett, A. *Int. J. Peptide Protein Res*. **1981**, *17*, 353−364.
(29) Holloway, P. W.; Mantsch, H. H. *Biochemistry* **1989**, *28*, 931−935.
(30) Le Tilly, V.; Sire, O.; Alpert, B.; Chinsky, L.; Turpin, P.-Y. *Biochemistry* **1991**, *30*, 7248−7253.
(31) Asher, S. A.; Larkin, P. J.; Teraoka, J. *Biochemistry* **1991**, *30*, 5944−5954.
(32) Copeland, R. A.; Spiro, T. G. *Biochemistry* **1985**, *24*, 4960−4968.

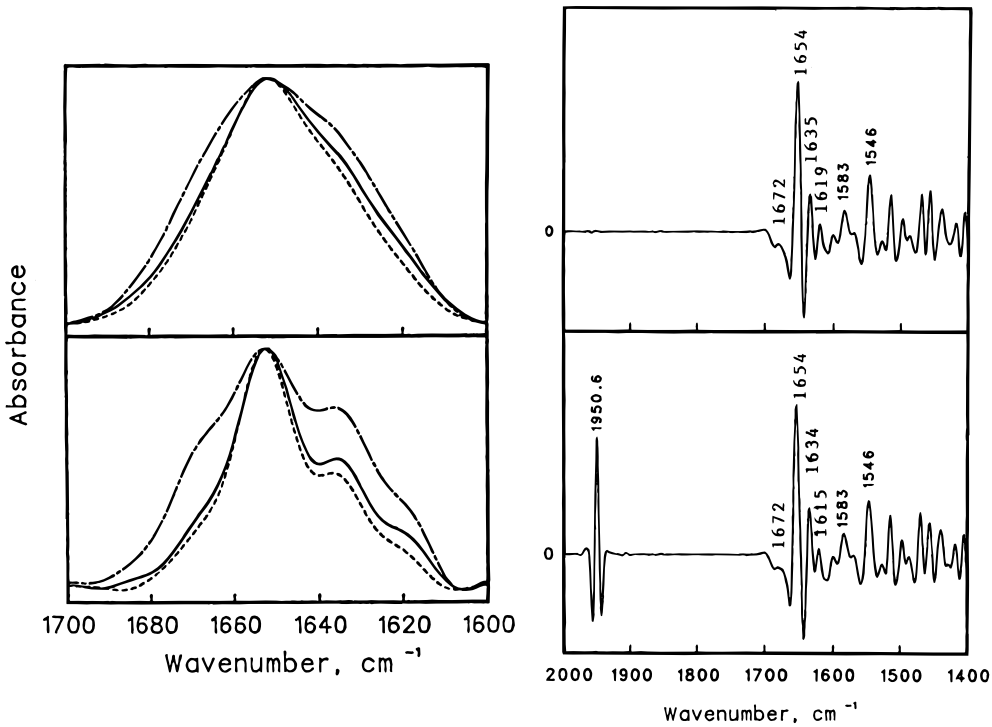

Figure 3. IR amide I′ band profiles of human hemoglobin. (Left, top): Spectra of (—) HbO_2, (- - -) HbCO, and (— · —) deoxyHb given for comparison. (Left, bottom): deconvoluted spectra obtained by Fourier self-deconvolution by using a 25 cm^{-1} band width and a resolution enhancement factor of 1.4. These deconvoluted spectra show the different components. (Right): Second derivative spectra of HbO_2 (top) and HbCO (bottom). The derivative was obtained by using a power of 3 and a breaking point of 0.3. The peak at 1950.6 cm^{-1} features the stretching band of CO bound to iron. Amide I′ components range from 1672 to 1615 cm^{-1}. The peaks at 1583 and 1546 cm^{-1} correspond to the amide II band. Experimental conditions are as follows: protein concentration 6 mM; path length 25 μm; 0.1 M bis-Tris, pD 7; 20 °C.

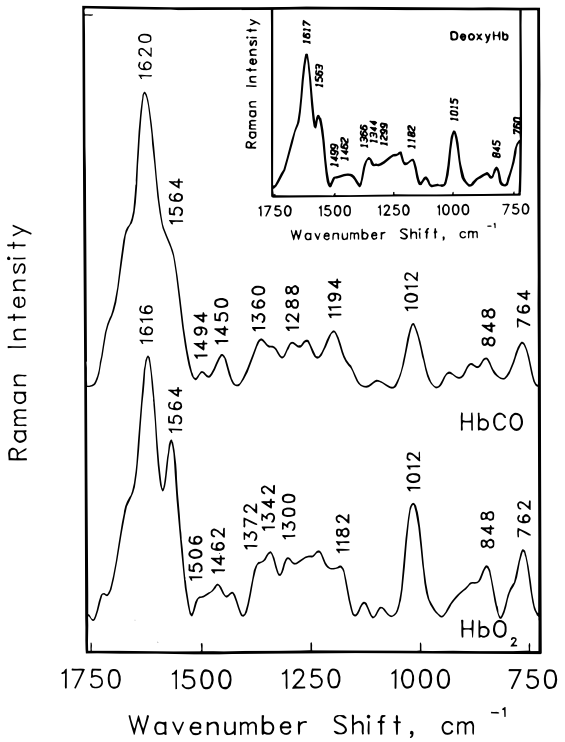

Figure 4. Iron−ligand effect on the UVRR spectrum of human hemoglobin: upper, HbCO; lower, HbO_2. The spectra have been vertically shifted for easier comparison between the two derivatives. Inset: Spectrum of deoxyHb. Experimental conditions are as follows: protein concentration 0.4 mM; 0.1 M bis-Tris, pH 7; $\lambda_{exc} = 223.6$ nm; 3 °C. Spectra are normalized on the water O−H stretching band (3450 cm^{-1}).

cm^{-1} (benzene and pyrrole in-phase ring breathing), the 1012 cm^{-1} band (benzene and pyrrole out-of-phase ring breathing), the 1342−1372 cm^{-1} doublet (ν_{14} and pyrrole), and the bands around 1462−1494 cm^{-1} ($\nu_{19a,b}$) and around 1564 cm^{-1} (naphtalene-like symmetric stretching), while Tyr residues contribute mainly to the bands around 1182 cm^{-1} (ν_{9a}) and around 1617 cm^{-1} (ν_{8a}).[33] In going from O_2 to CO, Trp intensity contributions at 1564, 1012, and 762 cm^{-1} largely decrease. Variations also occur in the Trp 1342−1372 and 1462−1494 cm^{-1} doublets. Another noticeable change is observed in the 1182−1194 cm^{-1} Tyr doublet (ν_{9a}, ν_{7a}).

The intensity ratio between the 1372 and 1342 cm^{-1} bands is thought to reflect the hydrophobicity around the indole ring of Trp β37.[34,35] Since this ratio is lower than one in HbO_2 and higher than one in HbCO, Trp β37 should be considered to be in a hydrophobic environment in HbCO, while it should be in a more polar or hydrophilic environment in HbO_2.[36] By contrast and despite the weak signal, given the higher intensity of the peak around 870 cm^{-1} in HbO_2 than in HbCO, it appears likely that the indole N_1H proton of Trp β37 forms a stronger H bond in HbO_2 as compared to HbCO.[34,37] This indicates that in both ligated hemoglobin forms, the H bond linking Trp β37 to Asp α94 residues is not totally broken,[38] but only highly reduced.

Since the Trp and Tyr residues are located far from the iron binding site, their Raman signals cannot reflect directly the structural organization of the heme-pocket domain. The Raman spectral modifications should mainly reflect changes in electric interactions inside the protein matrix. Indeed, with the 6 Trp and 12 Tyr residues of the hemoglobin tetramer being distributed at various distances from the iron sites, this should result in Raman band broadening if the corresponding bands are primarily

(33) Lord, R. C.; Miller, F. A. *J. Chem. Phys.* **1942**, *10*, 328−341.
(34) Harada, I.; Takeuchi, H. In *Spectroscopy of Biological Systems*; John Wiley: New York, 1986; pp 113−175.
(35) Nagai, M.; Kaminaka, S.; Ohba, Y.; Nagai, Y.; Mizutani, Y.; Kitagawa, T. *J. Biol. Chem.* **1995**, *270*, 1636−1642.
(36) Harada, I.; Miura, T.; Takeuchi, H. *Spectrochim. Acta Part A Mol. Spectrosc.* **1986**, *42*, 307−312.
(37) Miura, T.; Takeuchi, H.; Harada, I. *Biochemistry* **1988**, *27*, 88−94.
(38) Fung, L. W.-M.; Ho, C. *Biochemistry* **1975**, *14*, 2526−2535.

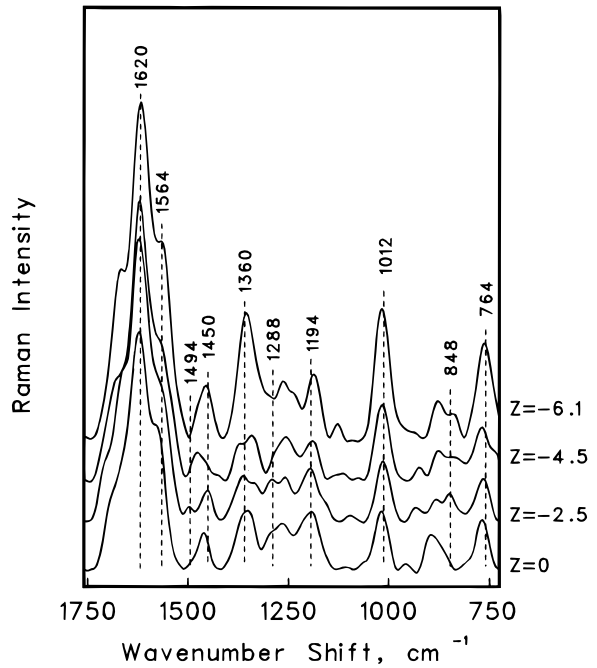

Figure 5. Protein charge effects on the UVRR spectrum of human HbCO. The spectra have been vertically shifted for easier comparison. *Z*, featuring the charge borne by the protein, is calculated from data in ref 39. From bottom to top, the corresponding pH values are 6.2, 7.0, 7.8, and 8.6. Vertical lines feature the peak positions of HbCO at pH 7.0 as shown in Figure 4.

altered by an electric field. This is actually observed. Thus, to probe the electrostatic remodeling within the protein, Raman spectra of HbCO were collected at four various pH values, allowing the charge borne by the protein to vary from $Z = 0$ to -6.1.[39] The evolution of the Raman spectra (Figure 5) as a function of *Z* reflects the intra-protein electric array changes.[39] A similar pH dependence has been previously reported for HbO_2[20] and for horse and sperm whale myoglobins.[30,31] This confirms that the particular electric field surrounding aromatic residues in human hemoglobin depends both on the protein charge and on the iron−ligand nature.

Discussion

From previous investigations, the difference in hemoglobin affinity for O_2 and CO was thought to only implicate iron−ligand bond geometry (ref 4 and articles therein, also ref 5) or the access of the ligand to the binding site.[3] More recently, emphasis has shifted to local polar constraints in the heme pocket. This has restricted consideration to the steric hindrance of the heme pocket and the residues located in close vicinity of the iron as the relevant parameters for the affinity variations in hemoglobin. Nevertheless, no correlation with the hemeprotein affinity has been observed.[6,7] The present work shows that the whole protein matrix is largely involved in the modulation of the hemoglobin affinity for its ligands. As expected the effects are quite small; yet the fact that they are even discernible in the FTIR, CD, and Raman data indicates that they are global.

The nature of the iron−ligand bond affects the repartition of the strains over the entire protein and at the subunit interfaces. If one assumes that the strength of these interactions is proportional to their infrared band intensity, the quaternary contacts inside the HbCO molecule will be weaker than those in the HbO_2 derivative. This agrees well with a previous infrared study on the β_{112} thiol,[39] which showed that interactions at the $\alpha_1\beta_1$ interface are stronger in HbO_2 than in HbCO. In addition, the small but discernible environment variation of the Trp β37 suggests that the flexible joint region (α_1FG−β_2C contact) of the $\alpha_1\beta_2$ interface[40] is also largely influenced by the iron−ligand nature.[38−41] Moreover, this work shows that the protein H-bond network is sensitive to the nature of the iron−ligand bond. The dipolar character of the H bonds is certainly responsible for their sensitivity to the electric field variation within the protein moiety. Thus, the totality of the strains distributed over the protein matrix should depend on the iron−ligand bond. Such an effect matches previous observations well: HbCO subunits exhibit stiffer H bonds than HbO_2.[39]

Upon O_2 ligand replacement by CO, electronic reorganization of the heme occurs and should produce a set of electrostatic interactions[42] which differ from the previous one. Thus, each iron−ligand bond should provide, without affecting the shape of the tetramer molecule, a particular charge distribution within the protein matrix. This hypothesis is well supported by previous NMR investigations which had shown that the ionization of several histidine residues (p*K* values) depends both on their location and on the nature of the iron−ligand bond: O_2 or CO.[43] Recent NMR studies point out the importance of these charges in the global electrostatic network of the protein.[44] NMR data and this work display that, thanks to its charge array, the entire protein matrix is involved in hemoglobin regulation mechanisms. The efficiency of Coulombic and polar interactions suggests that long-distance electrostatic couplings would be prominent factors for ligand affinity. They are also certainly responsible for the interactive properties of the hemoglobin molecule.[45] Tight electrostatic couplings between the heme−ligand complex and the protein matrix[42] should be responsible for the setting of the unique pattern of strains which accompanies the ligation change process. In this way, the whole matrix is sensitive to the chemical nature of the iron−ligand bond.

The new insights of this work associated with high-resolution NMR data reveal the surprising existence of connections between all the regions of the protein, as well as the strategic role played by the repartition of histidine residues in the multiple pathways used for signal communication.[46−48] This is one of the better examples of the global role of the protein matrix for its functional properties. Thus, long range electrostatic interactions would promote the energy transduction throughout the whole molecule. Accordingly, the conformational change, which occurs when hemoglobin switches from the R to the T form, can result from the very properties of the electrostatic interaction, which fulfill every requirement for allowing optimal energy transduction throughout the macromolecule.

Acknowledgment. The authors thank Prof. G. Weber (University of Illinois at Urbana−Champaign) for his interest in this work, his comments, and his suggestions. C.Z., S.P., and B.A. dedicate this study to his memory.

JA9703786

(39) El Antri, S.; Sire, O.; Alpert, B. *Eur. J. Biochem*. **1990**, *191*, 163−168.

(40) Baldwin, J.; Chothia, C. *J. Mol. Biol.* **1979**, *129*, 175−220.

(41) Ishimori, K.; Imai, K.; Miyazaki, G.; Kitagawa, T.; Wada, Y.; Morimoto, H.; Morishima, I. *Biochemistry* **1992**, *31*, 3256−3264.

(42) Matthew, J. B.; Hanania, G. I. H.; Gurd, F. R. N. *Biochemistry* **1979,** *18*, 1928−1936.

(43) Russu, I. M.; Ho, C. *Biochemistry* **1986**, *25*, 1706−1716.

(44) Sun, D. P.; Zou, M.; Ho, N. T.; Ho, C. *Biochemistry* **1997**, *36*, 6663−6673.

(45) Ho, C.; Russu, I. M. *Biochemistry* **1987**, *26*, 6299−6305.

(46) Stevens, R. C.; Lipscomb, W. N. *Proc. Natl. Acad. Sci. U.S.A.* **1992**, *89*, 5281−5285.

(47) Lipscomb, W. N *Adv. Enzymol.* **1994**, *68*, 67−151.

(48) Barrick, D.; Ho, N. T.; Simplaceanu, V.; Dahlquist, F. W.; Ho, C. *Nat. Struct. Biol.* **1997**, *4*, 78−83.

(49) Royer, C. A.; Beechem, J. M. *Methods Enzymol*. **1992**, *210*, 481−505.